Differential Phase Contrast X-Ray Microscopy

G. R. Morrison[1] and B. Niemann[2]

[1]Department of Physics, King's College, Strand, London WC2R 2LS, UK
[2]Georg-August-Universität Göttingen, Forschungseinrichtung Röntgenphysik, Geiststrasse 11, D-37073 Göttingen, Germany

Abstract. The advantages of using a configured detector to obtain differential phase contrast image in a scanning transmission X-ray microscope are described. A prototype system using a CCD detector has been installed on the microscopy beamline at BESSY, and the first images have been acquired.

1 Introduction

There is an increasing interest in the development of phase contrast imaging techniques at X-ray wavelengths. These techniques were often first applied in the context of visible light microscopy, and offer the possibility of improved image contrast, particularly when using relatively hard X-rays, or when operating on the low-energy side of an elemental absorption edge, since the phase information can provide complementary specimen information to that furnished by the usual X-ray absorption signal. It is the aim of this paper to describe a method of producing phase contrast X-ray images that can make very efficient use of the available illumination, and will also provide a very flexible set of imaging configurations that extend and enhance the performance of the microscope.

2 Phase Contrast Methods in X-Ray Microscopy

The advantages of using phase contrast techniques at X-ray wavelengths were first outlined by Schmahl et al. [1], and since then a number of different schemes have been developed. The first system to be realised was on the transmission X-ray microscope (TXM) at the BESSY synchrotron in Berlin [2], and involved the use of a phase-shifting plate in the back focal plane of the objective zone plate. This method is analogous to the Zernike method of phase contrast that has been in use in visible light microscopy for many years, with the exception that at X-ray wavelengths the phase plate will also attenuate the beams that pass through it. A form of phase contrast imaging is also possible using holographic techniques, since the hologram can, in principle, allow the reconstruction of both the amplitude and phase of the wave scattered by the object [3]. The importance of the phase term in producing image contrast when using coherent beams of 10–50 keV X-rays was recently demonstrated at the ESRF [4], where a simple in-line geometry was used to record the holographic images.

2.1 Configured Detectors in STXM

The reciprocity theorem, first outlined for the electron-optical equivalents of the TXM and the STXM [5], can be used to show that, under certain general conditions, the TXM and the STXM produce equivalent imaging conditions. However, the roles of the detector and the source are interchanged between the two instruments, and this has important consequences for the ease with which various imaging modes can be realised in the two instruments. Two examples illustrate very clearly the consequences of the different microscope geometries, when both the TXM and the STXM have the same objective focusing elements with the same diffraction-limited spatial resolution.

First, the spatial resolution actually achieved in an image produced by the TXM is the convolution of the diffraction-limited resolution with a function describing the resolution of the medium used to record the image, whereas in the STXM the spatial resolution is determined by the size of the focused X-ray probe incident on the sample, and this is given by the convolution of the diffraction-limited resolution with a function describing the finite size of the X-ray source. The TXM will achieve its highest possible resolution when the recording medium has a very fine grain, whereas the STXM requires a very small effective source to achieve the same result. Conversely, the size of the effective source in the TXM determines the degree of coherence of the illumination; a small source can lead to nearly coherent imaging conditions, while an extended source usually leads to incoherent imaging conditions. In the STXM, the use of an extended detector that collects all of the transmitted flux leads to incoherent imaging conditions, whereas coherent imaging conditions require the use of a detector that collects only a small fraction of the solid angle of illumination diverging from the specimen plane.

Although the STXM and TXM can produce equivalent imaging conditions, these examples show that one geometry can often result in a more efficient or effective way of realising a particular imaging condition. For example, the use of a detector with a small acceptance angle to produce coherent imaging conditions in a STXM discards all the information available in the rest of the transmitted flux and makes inefficient use of the available flux. The important point is that the two geometries are complementary, and should be used to realise different imaging modes in the most efficient manner possible. However, one particularly appealing feature of the STXM geometry is that the detector response function is (at least in principle) an instrumental parameter that is under the control of the user. The equivalent source intensity distribution in the TXM is, by definition, always a positive quantity. Since the detector response may be either positive or negative, it can be made to vary its functional form in ways that are completely impracticable for an X-ray source. This means that a number of novel imaging modes can be realised in the STXM that have no practical equivalent in the TXM. It is this that leads to the idea of 'configured detector' imaging in the STXM.

2.2 Theoretical Development of Configured Detector Imaging

A more detailed discussion of the theoretical development has already been published [6], so only a brief summary will be given here. The STXM detector plane is considered to be in the far field, where the complex amplitude in the detector plane is related by a Fourier transform to that on the specimen exit plane. Positions in the sample plane are given by vector $\mathbf{r}$, while positions in the plane of the detector are referred to by the spatial frequency vector $\mathbf{k}$. For an isoplanatic imaging system, and a specimen that can be described by a multiplicative amplitude transmittance $h(\mathbf{r})$, the complex amplitude of the transmitted wave at the exit surface of the specimen is

$$\psi(\mathbf{r}, \mathbf{r}_o) = \psi(\mathbf{r} - \mathbf{r}_o)h(\mathbf{r}) \tag{1}$$

when the focused probe is centred at $\mathbf{r}_o$. If $R(\mathbf{k})$ denotes the response function of the detector, then the detected signal is given by

$$s(\mathbf{r}_o) = \int |\Psi(\mathbf{k}, \mathbf{r}_o)|^2 R(\mathbf{k}) d\mathbf{k} \tag{2}$$

ignoring all irrelevant phase factors and constants outside the integral. $\Psi(\mathbf{k}, \mathbf{r}_o)$ is the Fourier transform of the wavefunction $\psi(\mathbf{r}, \mathbf{r}_o)$.

In the case of a weak-phase, weak-amplitude specimen the linear amplitude and phase contrast transfer functions for the imaging system can be written in the form

$$\mathcal{T}_a(\mathbf{k}) = \mathcal{C}(1, 0, \mathbf{k}) + \mathcal{C}(0, -1, \mathbf{k}) \tag{3}$$

$$\mathcal{T}_\phi(\mathbf{k}) = i[\mathcal{C}(1, 0, \mathbf{k}) - \mathcal{C}(0, -1, \mathbf{k})] \tag{4}$$

where

$$\mathcal{C}(m, n, \mathbf{k}) = \int \Psi(\mathbf{k}_1 - m\mathbf{k})\Psi^*(\mathbf{k}_1 - n\mathbf{k})R(\mathbf{k}_1)d\mathbf{k}_1 \tag{5}$$

Simple symmetry arguments show that, if the probe wave-function is aberration free, then $\mathcal{T}_\phi(\mathbf{k})$ vanishes when $R(\mathbf{k})$ is an even function of $\mathbf{k}$, and $\mathcal{T}_a(\mathbf{k})$ vanishes when $R(\mathbf{k})$ is an odd function. In principle, this means that it is possible to get a complete separation of the amplitude and phase information from the specimen by forming images with two different detector configurations, one with an even response, and one with an odd response. In the latter case the image is said to be in differential phase contrast (DPC), since the signal is proportional to the phase gradient of the specimen transmittance.

The ideal form of DPC detector is one that provides the first moment of the intensity distribution landing on it. This can be shown to have an unconditionally linear response to phase gradients [7]. The split detector, first proposed for use in the scanning transmission electron microscope [8], and opposite quadrant (OQ) detector configurations are easier DPC configurations to realise in practice, since they do not require a continuously varying detector response. Both configurations are available when the usual brightfield detector is dissected into four quadrants centred on the optical axis. Figure 1 shows a set of images illustrating a number of possible detector response functions, while Fig. 2 shows the corresponding contrast transfer functions.

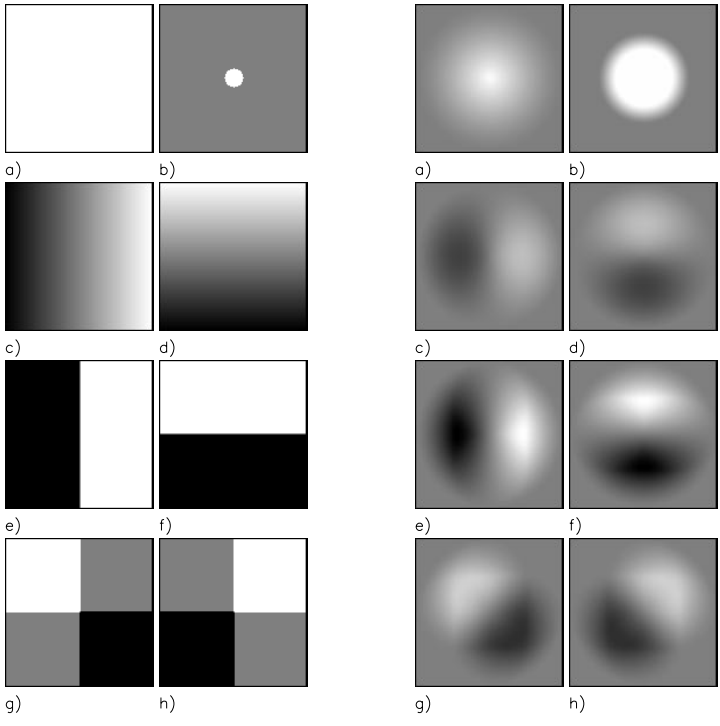

Fig. 1. *Left:* Images showing the response functions for a number of different detector configurations. Mid grey corresponds to a zero value, white to a value of +1 and black to a value of −1. a) Uniform detector for incoherent brightfield imaging. b) Uniform axial disk detector for partially coherent brightfield imaging. c) First moment detector sensitive to horizontal phase gradients. d) First moment detector sensitive to vertical phase gradients. e) Split detector sensitive to horizontal phase gradients. f) Split detector sensitive to vertical phase gradients. g) OQ detector sensitive to diagonal phase gradients. h) OQ detector sensitive to diagonal phase gradients (orthogonal to (g)).

Fig. 2. *Right:* Images showing the contrast transfer functions for the detector response functions shown in Fig. 1. The key to figures a) to h) is given in the caption for Fig. 1.

2.3 Practical Implementation of Configured Detector Systems

The usual mode of operating the STXM is for there to be a single detector downstream of the sample that collects all of the X-ray flux transmitted by the sample, producing an incoherent brightfield image where the contrast represents an X-ray absorption map of the sample. The basic requirement for a configured detector is that it can select only a fraction of the transmitted flux, but the advantage of using a multi-element detector in the STXM is that different detector response functions can be simulated after the image has been collected, simply by forming appropriate combinations of the signals from the various detectors.

This means that a number of different detector configurations are available simultaneously, and that a single scan of the specimen can provide sufficient data to analyse both the amplitude and phase terms of its complex transmittance.

Darkfield Imaging. A darkfield image is formed when only radiation scattered outside the brightfield cone is allowed to fall on the detector. This results in an image which has the maximum possible contrast, although the contrast is related non-linearly to the object transmittance. The first darkfield images were recorded simply by placing a stop in front of the usual STXM detector to occlude the brightfield cone [9], but more recent examples of the technique have also made use of a multi-element charge-coupled device (CCD) detector [10].

Quadrant Detector Imaging. The quadrant detector has been the form of configured detector most commonly used to produce differential phase contrast images in visible-light and electron microscopy. A practical system for X-ray microscopy requires that each quadrant is capable of high-speed photon counting, and that there be both the minimum dead space and the minimum of cross-talk between the four channels, while still maintaining the maximum uniformity of response. Solid-state avalanche photodiode detectors have been shown to be suitable for use with soft X-rays [11], but the quadrant version has been found to suffer from some problems with cross-talk that requires special signal processing electronics to deal with [12].

Configurable CCD Detector. The most flexible form of configurable detector is one that is divided into a large number of small X-ray-sensitive elements. Back-face thinned CCD detectors have now replaced photographic film as the recording medium of choice in almost all the current generation of TXM's, as they provide high detective quantum efficiency with the convenience of on-line electronic recording and visualisation of the image data [13]. In some senses such a CCD is also an ideal form of configurable detector for the STXM, but there are two main problems: the first is that the CCD arrays used in the TXM have typically 512^2 or 1024^2 pixels and the readout time for a full CCD frame is usually measured in seconds, the second is that a huge volume of data is generated by even a single image scan if a full CCD frame is recorded for each pixel position in the STXM image scan. Both problems can be alleviated if the individual cells are combined electronically at the readout stage to produce a smaller effective array size, but the CCD frame readout times are still too long to allow large raster sizes to be used for the STXM scan. Ideally, the CCD frame readout time should be no more than a few milliseconds.

Despite the present difficulties with using a CCD system as a detector in the STXM, one has been used on the STXM at the NSLS Brookhaven [10], initially as an aid to the alignment of the zone plate optics, and as a means of recording X-ray microdiffraction patterns. It has subsequently been used to record microdiffraction patterns for each pixel in the raster scan of STXM images, and these

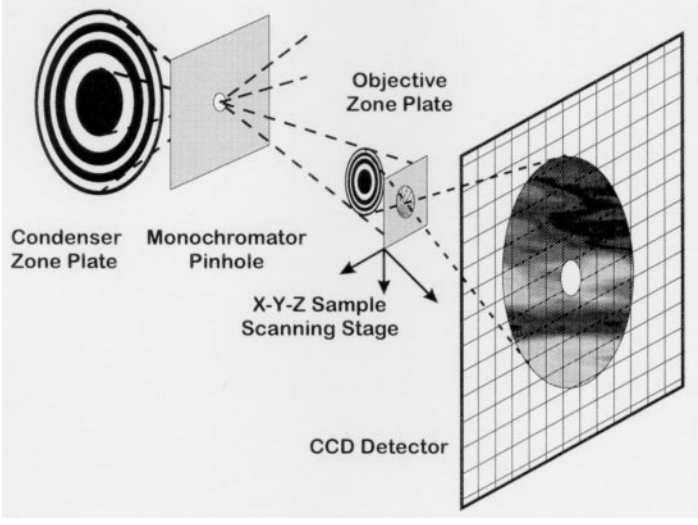

Fig. 3. Schematic diagram of the BESSY TXM converted to operate as a configured detector STXM

data have been used to reconstruct complex amplitude and phase maps of the specimen [14] using the method of Wigner-distribution deconvolution [15].

3 Configured Detector Imaging at BESSY

The Göttingen TXM at BESSY was the first to be fitted with a back-face thinned CCD detector to record full-field image data. Despite the relatively slow readout times offered by the CCD, it was decided to build a demountable scanning system that could be inserted into the existing TXM beamline to convert it into a prototype STXM. In particular, the aim was to assess the performance of the CCD system as a configurable detector, and to compare experimentally the image signals generated by various antisymmetric detector configurations.

3.1 Operation in STXM Mode

To accommodate the change to a STXM mode of operation the usual objective zone plate of the TXM was removed, and a scanning system, allowing 3-axis motion of the sample under stepper-motor control, was mounted inside the vacuum of the CCD camera chamber, as shown schematically in Fig. 3. A new, long focal length objective zone plate, with 200 nm resolution, was placed about 7 mm upstream of the sample. The objective zone plate produced a demagnified image of the monochromator pinhole on the sample plane and, in the absence of a sample, the diverging brightfield cone illuminated approximately half the available area of the CCD detector. Data collection was controlled by the existing acquisition software for the CCD (PMI software from Photomatrix), using

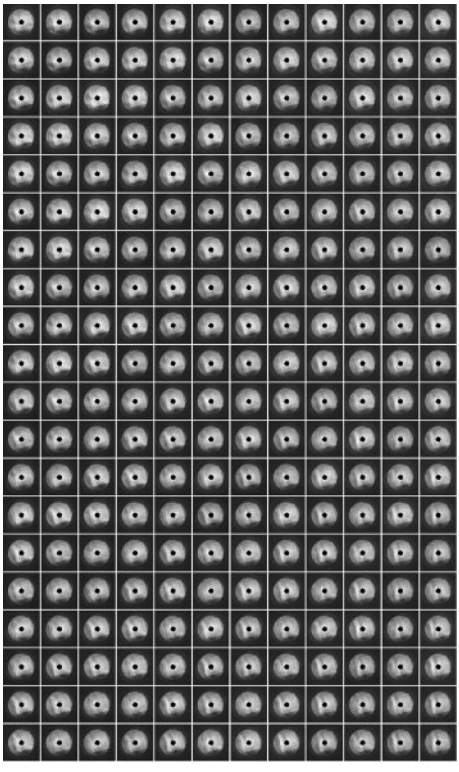

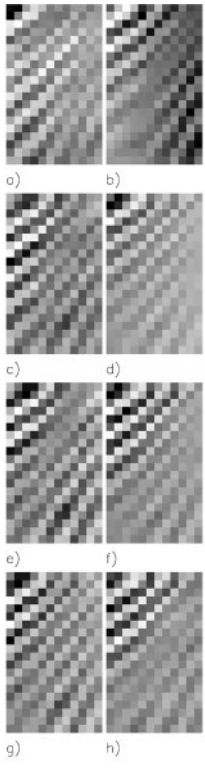

Fig. 4. *Left:* Each frame in this 12 by 20 raster shows the signal on the CCD detector for a single position in the STXM scan of a Simens star test pattern. The CCD dark background signal has been subtracted and the zero-order light from the objective zone plate has been masked off.

Fig. 5. *Right:* A set of configured detector images calculated from the data in Fig. 4. Each frame in Fig. 4 yields one pixel value for each image in Fig. 5a) to h), using the corresponding detector response functions shown in Fig. 1a) to h). The scan step between pixels was approximately 200 nm.

command macros to collect sequences of CCD frames at user-definable intervals. The microprocessor system that moved the scanning stage was triggered by the closure of a mechanical shutter in front of the detector, so that all sample motion took place during the readout phase of the CCD. The minimum interval between pixels was about 2s. To keep the data sets to a manageable size and to keep the overall acquisition times to a reasonable duration, the CCD frame was rebinned during the readout phase from a 1024^2 to a 64^2 array, and the STXM image scans were generally restricted to rasters of no more than 20 by 20 pixels.

An example of a STXM mode scan is shown in Fig. 4, which shows the full CCD frame recorded for each pixel position in a 12 by 20 scan of the sample. The scan step size was approximately 200 nm in both axes, and the specimen imaged

was part of a 19 μm diameter Simens star test pattern fabricated in 150 nm thick germanium on a 100 nm thick silicon nitride membrane by P.S. Charalambous at King's College London. Germanium has a relatively high ratio of the refractive index to the absorption index at the operating wavelength of around 2.4 nm, and the pattern consists of a series of 48 radial spokes, so it provides a continuously varying set of spatial periods that cover the expected resolution range of the imaging system. Although it is usual to operate an STXM with both a central stop on the zone plate and a order-selecting aperture between the zone plate and the sample, to eliminate undiffracted radiation and to prevent higher diffraction orders from reaching the detector plane, neither of these features was necessary when operating with the geometry shown in Fig. 3. In this case, the specimen was itself mounted across a 20 μm diameter pinhole which eliminated all but a narrow pencil of zero-order light coming through the centre of the zone plate. The active area of the CCD was 25 mm by 25 mm, so the zero-order pencil would illuminate only a few central cells of the detector, and it was straightforward to mask off the signal from these few CCD cells during the subsequent data processing phase, without significantly affecting the signal of interest from the brightfield cone.

A set of programs was written in the IDL programming language to read in image data such as that shown in Fig. 4, and then to calculate a number of possible image signals by weighting each of the CCD frames by different detector response functions, as shown in Fig. 1. These calculations take only a few seconds on a 120 MHz Pentium PC, and the resulting set of images could be displayed on the beamline immediately after the data acquisition. An example of such a set of configured detector images in shown in Fig. 5.

3.2 Interpretation of DPC Images

Each frame in Fig. 4 is effectively a convergent beam diffraction pattern from a different point in the test object, and a careful examination of the frames shows a rich variation in the intensity distribution across the detector plane that was very sensitive to the position of the focused probe. Indeed, it was noted during the alignment phase that a simple real-time observation of the CCD signal as the sample position was adjusted was remarkably effective in identifying when the sample was close to focus. The usual brightfield image signal, formed from the integrated intensity in each CCD frame, is insensitive to much of this information. A smaller brightfield detector produces partially coherent imaging conditions, but there will be no phase contrast in the absence of lens aberrations, and the spatial resolution is poorer because the contrast transfer function is narrower. Antisymmetric detector configurations produce phase contrast from the information they give on the redistribution of intensity across the detector plane, and they can do this without sacrificing resolution. However, the DPC signal has a directional dependence, so that there will be little or no information transfer for some features in the object. At X-ray wavelengths, strong phase gradients, are usually accompanied by strong absorption gradients that can give image contrast if the sample is out of focus. Clearly, at least two independent

DPC images must always be examined, while the incoherent brightfield image can provide complementary information on the absorption contrast.

4 Conclusions

The use of a CCD detector provides a completely configurable form of detector that can be used in the STXM. As such it can provide a wealth of specimen information that is not available when a single brightfield detector is used. The additional information can be exploited by sophisticated analyses such the Wigner-distribution deconvolution method, but the degree of processing such techniques require means that they cannot presently be applied in real time. However, the use of a few simple antisymmetric detector configurations in addition to the usual brightfield combination allows real-time observation of the sample in both amplitude and phase contrast. Significant reductions in the volume of data generated during routine operation could be achieved if only the processed image data (for example, brightfield and two independent DPC signals) is stored, although the likely future availability of high-capacity, low-cost storage media may make this an unnecessary economy. The main technical challenge that needs to be addressed is the speed at which each frame of data is read from the CCD detector. Devices with 1024^2 pixels are excellent for imaging applications, but the requirement for STXM operation is for a much smaller array ($\approx 64^2$ is quite adequate) that can be read out at frame rates $\approx 1\,\mathrm{kHz}$. Fortunately, there is good reason to believe that such devices are soon to become readily available.

Acknowledgments

It is a pleasure to acknowledge the support provided by the research groups at King's College London and at Georg-August Universität Göttingen. Particular thanks are due to P. Guttmann, M. Peuker, T. Wilhein, M.T. Browne, and P.S. Charalambous.

References

1. Rudolph, D., Schmahl, G., Niemann, B.: Amplitude and phase contrast in X-ray microscopy. In: Duke, P.J., Michette, A.G. (eds.): Modern Microscopies. Plenum, New York 1990 pp.59–67
2. Schmahl, G., Rudolph, D., Schneider, G., Guttmann, P., Niemann, B.: Phase contrast X-ray microscopy studies. Optik **97** (1994) 181–182
3. McNulty, I.: The future of X-ray holography. Nucl. Inst. Meth. Phys. Res. A **347** (1994) 170–176
4. Snigirev, A., Snigireva, I., Kohn, V., Kuznetsov, A., Schelokov, I.: On the possibilities of X-ray phase-contrast microimaging by coherent high-energy synchrotron radiation. Rev. Sci. Instrum. **66** (1995) 5486–5492

5. Zeitler, E., Thomson, M.G.R.: Scanning transmission electron microscopy I and II. Optik **31** (1970) 258–280, and 359–366
6. Morrison, G.R.: X-ray imaging with a configured detector. In: Aristov, V.V., Erko, A.I. (eds.): X-ray Microscopy IV. Bogorodski Pechatnik, Chernogolovka 1994 pp.479–484
7. Waddell, E.M., Chapman, J.N.: Linear imaging of strong phase objects using asymmetrical detectors in STEM. Optik **54** (1979) 83–96
8. Dekkers,, N.H.de Lang, H.: Differential phase contrast in a STEM. Optik **41** (1974) 452–456
9. Morrison, G.R., Browne, M.T.: Darkfield imaging with the scanning transmission X-ray microscope. Rev. Sci. Instrum. **63** (1992) 611–614
10. Chapman, H.N., Jacobsen, C.J., Williams, S.: A characterisation of dark-field imaging of colloidal gold labels in a scanning transmission X-ray microscope. Ultramicroscopy **62** (1996) 191–213
11. Palmer, J.R., Morrison, G.R.: The use of avalanche photodiodes for the detection of soft X-rays. Rev. Sci. Instrum. **63** (1992) 828–831
12. Browne, M.T., Morrison, G.R.: A 100ns anti-coincidence circuit for multi-channel counting systems. Measurement Science and Technology **6** (1995) 1487–1491
13. Wilhein, T., Rothweiler, D., Tusche, A., Scholze, F., Meyer-Ilse, W.: Thinned, back-illuminated CCDs for X-ray microscopy. In: Aristov, V.V., Erko, A.I. (eds.): X-ray Microscopy IV. Bogorodski Pechatnik, Chernogolovka 1994 pp.470–474
14. Chapman, H.N.: Phase-retrieval X-ray microscopy by Wigner distribution deconvolution. Ultramicroscopy **66** (1996) 153–172
15. Rodenburg, J.M., Bates, R.H.T.: The theory of super-resolution electron microscopy via Wigner-distribution deconvolution. Phil. Trans. R. Soc. Lond. A **339** (1992) 521–553